RSC Pharmaceutics

ROYAL SOCIETY OF CHEMISTRY

PAPER

View Article Online
View Journal

Cite this: DOI: 10.1039/d6pm00045b

Chitosan-coated cobalt ferrite nanocomplexes with dual antimicrobial activity and hemocompatibility

Md Salman Shakil,[a] Shakil Ahmed Polash,[b] Md. Monir Hossain,[b] Mahruba Sultana Niloy,[c] Mohammad Mahfuz Ali Khan Shawan,[c] Sheikh Manjura Hoque, *[d] Md. Ashraful Hasan*[c] and Satya Ranjan Sarker [b]

The escalating prevalence of antibiotic-resistant bacterial infections represents a critical global health challenge, necessitating the development of alternative antimicrobial strategies that are both effective and biocompatible. Nanomaterials offer a versatile platform in this regard, as their physicochemical properties can be tailored to enhance antibacterial performance. Among these, cobalt ferrite nanoparticles (CFs) exhibit attractive magnetic properties, chemical stability, and multifunctionality for biomedical applications; however, their clinical translation is hindered by aggregation, limited colloidal stability, and potential biocompatibility concerns. Building on our previous work demonstrating the biocompatibility and imaging potential of chitosan (CH)-coated CFs (CCFs), this study investigates their antibacterial efficacy against a diverse panel of Gram-positive (*Bacillus subtilis* RBW and *Staphylococcus aureus*) and Gram-negative bacteria (enteropathogenic *Escherichia coli* EPEC, *E. coli* DH5α, *E. coli* K-12, *Salmonella typhi* AF-4500, *Shigella flexneri* 3C, and *Vibrio cholerae*). Antibacterial activity was evaluated using the zone of inhibition (ZOI), minimum inhibitory concentration (MIC), and CellTox™ Green assays. CCFs demonstrated significantly enhanced antibacterial activity compared to CH alone or uncoated CFs, highlighting the synergistic contribution of the chitosan coating. Notably, *S. aureus* exhibited the highest susceptibility, with a maximum ZOI of ~26.45 mm at 500 μg of CCFs. Elevated levels of malondialdehyde–thiobarbituric acid adducts following treatment suggest that membrane oxidative damage is a key mechanism underlying bacterial killing. Importantly, hemocompatibility assessments using rat and human erythrocytes revealed concentration-dependent cytotoxicity, indicating that CCFs maintain acceptable blood compatibility within a defined concentration range. Collectively, this study establishes CCFs as a promising dual-functional platform combining potent broad-spectrum antimicrobial activity with tunable hemocompatibility, underscoring their potential for future biomedical applications, provided that an optimal therapeutic window is carefully defined.

Received 1st February 2026,
Accepted 13th April 2026

DOI: 10.1039/d6pm00045b

rsc.li/RSCPharma

1. Introduction

The global rise of infectious diseases, compounded by the emergence of antibiotic-resistant Gram-positive and Gram-negative bacteria, poses a major public health challenge.[1,2] This threat is further aggravated by the decline in new antibiotic approvals over the past decade,[3] leaving common pathogens such as *Staphylococcus aureus*, *Enterococcus faecalis*, *Escherichia coli* EPEC, *Salmonella typhi* AF-4500, *Shigella flexneri* 3C, and *Vibrio cholerae* increasingly difficult to treat.[4–9] The growing antibiotic resistance of these bacteria underscores the urgent need for safe and effective alternative therapeutics.[2,10] Metal nanoparticles have emerged as promising antimicrobial agents due to their ability to disrupt bacterial membranes and limit resistance development pathways.[11,12]

Among the magnetic nanoparticles, cobalt ferrite nanoparticles (CFs), a class of spinel-type ferrites, possess unique magnetic and physicochemical properties that enable applications in magnetic resonance imaging (MRI) contrast enhancement, hyperthermia, targeted drug delivery, and antimicrobial therapy.[13–15] However, their biomedical application is often limited by particle agglomeration, poor aqueous dis-

[a]*Department of Microbiology, Brac University, Kha 224 Pragati Sarani, Merul Badda, Dhaka 1212, Bangladesh*
[b]*Department of Biotechnology and Genetic Engineering, Jahangirnagar University, Savar, Dhaka 1342, Bangladesh. E-mail: satya.sarker@bgeju.edu.bd*
[c]*Department of Biochemistry and Molecular Biology, Jahangirnagar University, Savar, Dhaka 1342, Bangladesh. E-mail: ashrafulhasan@juniv.edu*
[d]*Material Science Division, Atomic Energy Centre, Dhaka 1000, Bangladesh*

persibility, and potential cytotoxicity. To address these limitations, surface modification has been widely explored as an effective strategy to improve their biological performance.

Chitosan (CH), a natural, biocompatible polymer,[16,17] is particularly attractive for this purpose due to its broad applications in gene delivery, wound healing, tissue engineering and antimicrobial formulations.[18] Beyond serving as a stabilizing coating, CH can improve nanoparticle dispersion, target specificity, and biological interactions while reducing aggregation and clearance by the reticuloendothelial system.[12,19,20] Previous studies have also shown that CH may enhance the antimicrobial activity of CF-based nanomaterials.[21,22] Moreover, CFs, CH, and CH-coated CFs (CCFs) have each been reported to possess antimicrobial potential.[19,22–25] However, a comparative evaluation of their antimicrobial performance against commercially available FDA-approved antibiotics (*e.g.* ampicillin, tetracycline, ciprofloxacin) or disinfectant (*e.g.* povidone iodine) remains limited. The effects of CCFs on bacterial membrane lipid peroxidation and their hemocompatibility toward human red blood cells (HRBCs) have also not been investigated thoroughly. Such investigation is important for understanding both the antimicrobial potential and the future translational relevance of CCFs.

In the present study, we report the synthesis of CH-coated CFs by a co-precipitation method[26] and systematically evaluate their antibacterial activity against Gram-positive (*B. subtilis*, *S. aureus*) and Gram-negative (*E. coli* EPEC, *E. coli* DH5α, *S. typhi* AF-4500, *S. flexneri* 3C, *V. cholerae*, and *E. coli* K-12) bacterial strains. Their antimicrobial efficacy was compared with commercially available antibiotics by measuring the zone of inhibition (ZOI), the clear circular region surrounding an antimicrobial agent where bacterial growth is suppressed. Additionally, we examined the bacterial membrane damage through lipid peroxidation analysis and evaluated the hemocompatibility of CFs and CCFs toward HRBCs. Taken together, this study explores the antimicrobial potential of CCFs while also assessing their hemocompatibility in a concentration-dependent manner, thereby providing a more balanced evaluation of their biomedical applicability.

2. Materials and methods

2.1 Chemicals and materials

Peptone, yeast extract, sodium chloride, and EDTA were collected from UNI-CHEM, China. Mueller Hinton Agar was obtained from Merk, Germany. *Enterococcus faecalis*, *Staphylococcus aureus*, Enteropathogenic *Escherichia coli (EPEC)*, *Salmonella typhi AF-4500*, *Shigella flexneri 3C*, *Vibrio cholera*, and *Escherichia coli K-12* were obtained from the department of Biochemistry and Molecular Biology, Jahangirnagar University, Savar, Dhaka 1342, Bangladesh. *Escherichia coli DH5α* and *Bacillus subtilis RBW* were obtained from the department of Biotechnology and Genetic Engineering, Jahangirnagar University, Savar, Dhaka 1342, Bangladesh.

2.2 Methods

2.2.1 Synthesis and characterization. CFs and CCF nanocomplexes were synthesized and characterized as described previously by Shakil *et al.*[26] Briefly, $FeCl_3{\cdot}6H_2O$ (Merck, India, impurity ≤0.01%) and $CoCl_2{\cdot}6H_2O$ (Merck, India, impurity ≤0.01%) were mixed in the required molar ratio, and 6 M NaOH was added dropwise under constant stirring to maintain the pH at 11–13, resulting in precipitation. The precipitate was separated by centrifugation (15 000 rpm, 20 min), washed ten times, and annealed at 90 °C for 72 h to obtain the CFs.

$$CoCl_2{\cdot}6H_2O + 2NaOH \rightarrow Co(OH)_2 + 2NaCl + 6H_2O$$

$$2FeCl_3{\cdot}6H_2O + 6NaOH \rightarrow 2Fe(OH)_3 + 6NaCl + 12H_2O$$

$$Co(OH)_2 + 2Fe(OH)_3 \rightarrow CoFe_2O_4 + 4H_2O$$

Overall reaction:

$$CoCl_2{\cdot}6H_2O + 8NaOH + 2FeCl_3{\cdot}6H_2O \rightarrow CoFe_2O_4 + 8NaCl + 22H_2O$$

CFs were then coated using a 2% CH solution to prepare CCFs. 2% CH (w/v) was prepared by adding CH (Sigma-Aldrich, low molecular weight, quality level 100, 75–85% deacetylated) into a mixture of water (94 mL) and an acetic acid solution (6 mL, Sigma-Aldrich, 2 N). After 48 h of stirring, the CH solution was centrifuged for 20 minutes at 13 000 rpm. 1 mL of the clear supernatant was then used to coat 20 mg CFs *via* repeated vortexing and ultrasonication.

2.2.2 Antimicrobial activity assay. The antibacterial activities of CH, CFs, and CCFs were investigated by the disc diffusion method according to Niloy *et al.*[27] with slight modifications. Briefly, selected Gram-positive bacteria (*Bacillus subtilis* RBW, *Enterococcus faecalis*, and *Staphylococcus aureus*) and Gram-negative bacteria (*Escherichia coli* DH5α, enteropathogenic *E. coli* (EPEC), *Salmonella typhi* AF-4500, *Shigella flexneri* 3C, *Vibrio cholerae*, and *E. coli* K-12) were cultured overnight in Luria–Bertani (LB) broth at 37 °C with shaking at 120 rpm. Subsequently, 100 μL of each bacterial suspension was uniformly spread onto Mueller–Hinton agar (MHA) plates. Sterile filter paper discs impregnated with the test samples at concentrations of 300, 400, and 500 μg were placed on the inoculated plates, which were then incubated at 37 °C for 15 h,[28] while ampicillin, tetracycline, ciprofloxacin, and povidone iodine were used as positive controls. Antibacterial activity was assessed by measuring the diameter of the clear ZOI (mm) using slide calipers.

Minimum inhibitory concentration (MIC) value was determined using the broth dilution method.[27] Overnight bacterial cultures (10 μL) were diluted in 990 μL fresh LB broth and incubated at 37 °C with shaking (120 rpm) for 4 h. The cultures were then treated with a range of CH, CF, and CCF concentrations and incubated overnight. Bacterial growth was assessed by measuring OD_{600} using a UV-vis spectrophotometer to determine MIC values.

2.2.3 Trypan blue dye exclusion test. The trypan blue dye exclusion assay was used to determine the number of viable cells in a bacterial suspension.[29] Trypan blue is a negatively charged dye that selectively stains dead bacterial cells, while viable cells with intact membranes exclude the dye.[30] The assay was performed according to Sarker *et al.* with minor modifications.[31] Briefly, 20 μL of the sample (1 μg μL^{-1}) was mixed with 80 μL of an overnight-grown bacterial culture and incubated at 37 °C with shaking at 120 rpm for 1.5 h. Following treatment with CH, CFs, and CCFs, the bacterial cultures were mixed with 0.4% trypan blue solution and incubated at room temperature for 15 min. Images were then captured using a phase-contrast microscope (Olympus BX50 fluorescence microscope, Olympus, Japan) at 40× magnification.

2.2.4 CellTox™ Green assay. CellTox™ Green fluorescent dye penetrates cells with compromised membranes and emits green fluorescence upon binding to DNA.[32] The samples (20 μL; 1 μg μL^{-1}) were mixed separately with 80 μL of the respective bacterial cultures. Subsequently, 900 μL of fresh medium was added to the CH-, CF-, and CCF-treated bacterial suspensions, followed by incubation at 37 °C with shaking at 120 rpm for 2 h. After incubation, 1 μL of CellTox™ Green reagent (2×) was added to each sample, mixed thoroughly, and incubated for 30 min in the dark at room temperature. A 20 μL aliquot of the stained bacterial culture was used to visualize dead cells under a fluorescence microscope (Olympus BX50, Olympus, Japan). The fluorescence intensity of the remaining samples was measured using a spectrofluorophotometer (Shimadzu RF-6000, Japan) with excitation at 490 nm.

2.2.5 Lipid peroxidation (LPO) assay. The LPO assay was performed following the method of Sarker *et al.*[31] Briefly, 1 mL of bacterial culture was mixed with 200 μL (200 μg) of CFs, CH, or CCFs and incubated at room temperature for 2 h. After incubation, the cultures were centrifuged, and 2 mL of 10% trichloroacetic acid was added. Insoluble cellular components were removed by centrifugation at 11 000 rpm for 35 min. The supernatant was collected and centrifuged again at the same speed for 20 min to remove residual protein precipitates and dead cells. The resulting supernatant, containing malondialdehyde (MDA), was mixed with 4 mL of freshly prepared 0.67% thiobarbituric acid (TBA) solution and incubated in a hot water bath for 10 min to allow the formation of the MDA–TBA adduct. After cooling to room temperature, the absorbance of the MDA–TBA complex was measured at 532 nm using a UV-vis spectrophotometer (Specord® 205, Analytik Jena, Germany).

2.2.6 Hemolytic activity assay. The hemolytic activity of CH, CFs, and CCFs was evaluated following the method of Hossain *et al.* with slight modifications.[33] Whole blood was collected from a healthy male volunteer (25 years) and from male albino Wistar rats (7 weeks old) into tubes containing 10% EDTA and centrifuged at 5000 rpm for 10 min to remove the serum. The HRBCs and rat red blood cells (RRBCs) were then washed multiple times with phosphate-buffered saline (PBS) by centrifugation at 3000 rpm for 3 min and resuspended in 10 mL of PBS. Subsequently, 300 μL of the red blood cell (RBC) suspension was mixed with 1200 μL of CH-, CF-, or CCF-containing solutions. The final concentrations of the solutions were 50, 100, 150, 200, 250, 300, 350, and 450 μg mL^{-1}. The mixtures were incubated at 37 °C with stirring at 150 rpm for 30 min, followed by centrifugation at 4000 rpm for 5 min. The absorbance of the supernatants was measured at 570 nm. Positive (RBCs with distilled water) and negative (RBCs with PBS) controls were included, and percentage hemolysis was calculated using the following formula:

$$\%\ \text{Hemolysis} = \frac{(\text{sample absorbance} - \text{negative control absorbance})}{(\text{positive control absorbance} - \text{negative control absorbance})} \times 100.$$

2.2.7 Statistical analysis. Experimental data were analyzed using Prism-GraphPad 8 (USA). Data were represented as the mean ± standard error of the mean (SEM). Additionally, a one-way ANOVA coupled with a Bonferroni *post-hoc* test was used to determine a statistically significant difference at $P < 0.05$.

3. Results and discussion

3.1 Characterization

Previously synthesized CFs (diameter ~10 nm) were used in this study.[26] The surface of the CFs was modified with CH to improve their biocompatibility for potential biomedical applications. Briefly, CFs were prepared *via* the co-precipitation method and subsequently coated with CH. The resulting CCFs were characterized using scanning transmission electron microscopy (STEM), Raman spectroscopy, Fourier-transform infrared (FTIR) spectroscopy, differential scanning calorimetry (DSC), thermogravimetric analysis (TGA), dynamic light scattering (DLS), and zeta (ζ) potential measurements. CCFs exhibited higher positive surface charges than CH or CFs alone (Table S1).[26] In the present study, we evaluated the antimicrobial activity of CH, CFs, and CCFs against two Gram-positive and seven Gram-negative bacterial strains.

3.2 Antimicrobial activity

The disc diffusion assay was performed to evaluate the antibacterial activity of CH, CFs, and CCFs. CFs alone exhibited poor antimicrobial activity (Table 1), whereas CH coating substantially enhanced their efficacy. The highest activity of CCFs was observed against the Gram-positive *Staphylococcus aureus* strain (Table 1), outperforming even commercially available FDA-approved antimicrobial agents, including ampicillin, tetracycline, ciprofloxacin and povidone iodine. In contrast, CCFs were less effective against *Bacillus subtilis* RBW. Povidone iodine demonstrated nearly uniform antibacterial activity across all tested strains. Interestingly, CCFs also showed activity against amoxicillin-resistant Gram-negative *Escherichia coli* EPEC. Consistent with the zones of inhibition, MIC measurements indicated that CCFs (0.000391–0.000781 μg) were more potent than CH or CFs, while CFs and CH displayed

Table 1 Zones of inhibition (in millimeters) exhibited by CH, CFs, and CCFs against bacterial strains

Drug/Drug candidates	Bacterial strain								
	Bacillus subtilis RBW	*Escherichia coli* DH5α	Enteropathogenic *Escherichia coli* (EPEC)	*Salmonella typhi* AF-4500	*Shigella flexneri* 3C	*Vibrio cholerae*	*Escherichia coli* K-12	*Enterococcus faecalis*	*Staphylococcus aureus*
CH (300 μg)	—	7.45 ± 0.05	—	7 ± 0	7.05 ± 0	7.1 ± 0.1	7.45 ± 0.05	18.7 ± 0.2	20.5 ± 0.2
CH (400 μg)	6.9 ± 0.1	7.85 ± 0.05	—	7.45 ± 0.05	7.45 ± 0.05	8.05 ± 0.05	7.55 ± 0.05	20.55 ± 0.25	22.4 ± 0.1
CH (500 μg)	7.05 ± 0.05	8.15 ± 0.05	7.45 ± 0.05	8.05 ± 0.05	8.1 ± 0.05	9.9 ± 0.1	10.05 ± 0.05	21.7 ± 0.4	24.25 ± 0.15
CFs (300 μg)	6.9 ± 0.1	—	—	—	—	—	—	—	—
CFs (400 μg)	7 ± 0	—	—	—	—	—	—	—	—
CFs (500 μg)	7.1 ± 0.1	—	—	—	7.45 ± 0.05	—	—	8.05 ± 0.15	—
CCFs (300 μg)	7.45 ± 0.05	15.4 ± 0.1	8.55 ± 0.05	9.05 ± 0.05	6.9 ± 0.1	9.05 ± 0.05	8.05 ± 0.05	18.15 ± 0.05	21.1 ± 0.3
CCFs (400 μg)	9.05 ± 0.05	17.1 ± 0.1	10.05 ± 0.05	10.1 ± 0.1	9.45 ± 0.05	9.95 ± 0.05	8.95 ± 0.05	19.55 ± 0.15	23.45 ± 0.65
CCFs (500 μg)	9.1 ± 0.1	20.05 ± 0.05	12.015 ± 0.015	11.1 ± 0.1	11.05 ± 0.05	11.4 ± 0.1	11.1 ± 0.1	23.55 ± 0.05	26.45 ± 0.05
Ampicillin (10 μg)	10.95 ± 0.05	12.9 ± 0.1	—	23.95 ± 0.05	23.1 ± 0.1	14.2 ± 0.1	15.9 ± 0.1	7.95 ± 0.15	8.35 ± 0.15
Tetracycline (10 μg)	17.15 ± 0.15	17.1 ± 0.1	20.05 ± 0.05	15.1 ± 0.1	19.95 ± 0.05	8.1 ± 0.1	17.1 ± 0.1	12.3 ± 0.1	11.45 ± 0.05
Ciprofloxacin (5 μg)	24.9 ± 0.1	34.2 ± 0.1	36.9 ± 0.1	38.9 ± 0.1	32.05 ± 0.05	22.05 ± 0.05	29.4 ± 0.05	19.35 ± 0.15	19.35 ± 0.15
Povidone iodine (2000 μg)	10.1 ± 0.1	10.95 ± 0.05	9.55 ± 0.05	10.45 ± 0.05	10.5 ± 0	10.05 ± 0.05	12.05 ± 0.05	19.55 ± 0.15	17.4 ± 0.2

CFs: cobalt ferrite nanoparticles, CH: chitosan, CCFs: chitosan-coated cobalt ferrite nanoparticles.

similar MIC values (0.0125 μg) against *E. coli* DH5α, *E. faecalis*, *S. aureus*, and *E. coli* K12 (Table S1). Previously, Kajani *et al.*[34] reported that CCFs had higher antibacterial activity against *E. coli* than CFs or amoxicillin. The enhanced antimicrobial activity of CCFs is likely attributable to increased ROS production,[19] while CH coating promotes the attachment of CCFs to the bacterial cell wall or membrane, facilitating cell lysis.[35]

3.3 Compromised bacterial cell membrane

CellTox™ Green is a DNA-binding dye that penetrates bacteria with compromised cell walls, while intact bacterial membranes exclude the dye.[36] Among the Gram-positive bacteria, *S. aureus* treated with CCFs exhibited the highest fluorescence intensity, followed by *E. faecalis* (Fig. 1), with intensities approximately sevenfold higher than those of untreated controls. All Gram-negative strains showed nearly sixfold increases in fluorescence compared with their respective untreated controls. A significant increase in fluorescence was also observed in CCF-treated Gram-positive and Gram-negative bacteria compared with the untreated group and CF- and CH-treated groups. These results are consistent with the zones of inhibition data (Fig. 2). Green fluorescence of dead bacteria treated with CH, CFs, and CCFs was further confirmed under fluorescence microscopy (Fig. 2), with the highest level of cell death observed following CCF treatment. Previously, it has been reported that treatment with biogenic metal nanoparticles compromised the bacterial membrane, leading to an increase in the uptake of CellTox™ Green and fluorescence.[27,37]

The trypan blue dye exclusion assay confirmed bacterial cell wall damage. Hydrophobic interactions between the nanoparticles and the bacterial cell wall caused structural disruption, allowing trypan blue to penetrate the cytosol of damaged or dead bacteria.[38] Cells with compromised walls appeared blue under a phase-contrast microscope (Fig. S1).

3.4 Lipid peroxidation of the bacterial membrane

The LPO assay was performed to assess the oxidative damage to bacterial cell membrane fatty acids. The formation of the MDA–TBA adduct indicates cell wall damage induced by the therapeutic agents. Among the tested strains, treatment of *S. aureus* with CCFs resulted in the highest MDA–TBA adduct formation (Fig. 3a). Notably, *E. faecalis* also exhibited substantial MDA–TBA levels, indicating significant oxidative damage among the Gram-positive bacteria with CCFs (Fig. 3a). Previously, it has been reported that cobalt or iron doping in silver nanoparticles increased MDA adduct formation in both Gram-positive bacteria (*E. faecalis* and *B. subtilis*) and Gram-negative bacteria (*E. cloacae* and *Pseudomonas putida*).[39]

The composition of bacterial cell walls varies between species, resulting in different interactions with the test samples.[40] Consequently, different bacterial strains produced varying amounts of MDA–TBA adducts following treatment. LPO occurred due to the oxidation of bacterial cell membrane fatty acids induced by CH, CFs, or CCFs.

Positive surface charge of CH, CFs or CCFs could facilitate their interaction with negatively charged bacterial cell mem-

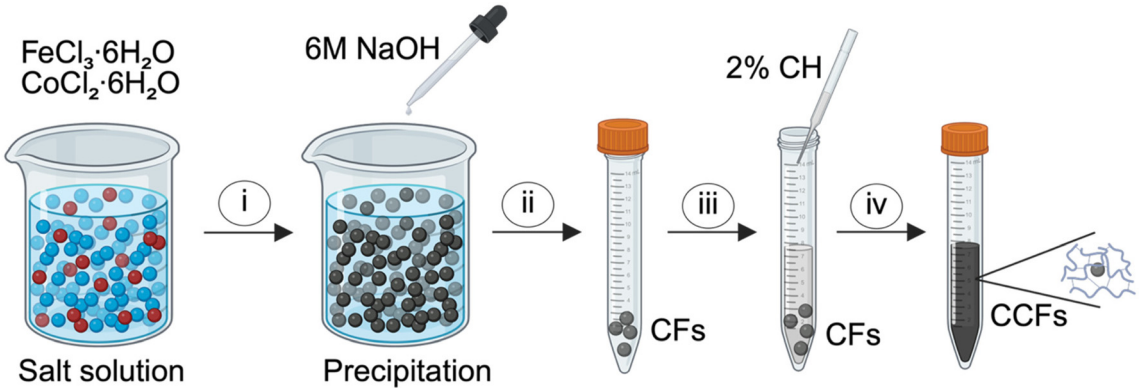

Fig. 1 Schematic representation of the synthesis of CCFs. $FeCl_3 \cdot 6H_2O$ and $CoCl_2 \cdot 6H_2O$ were dissolved in a beaker under constant stirring. Then, NaOH was added to initiate CF synthesis (i). Following precipitation, CFs were purified by washing and drying (ii). A 2% CH solution was then added to CFs (iii), and CFs were coated *via* repeated sonication and vortexing (iv). CFs: cobalt ferrite nanoparticles; CH: chitosan; CCFs: chitosan-coated cobalt ferrite nanoparticles. The illustration was created using BioRender (https://www.biorender.com).

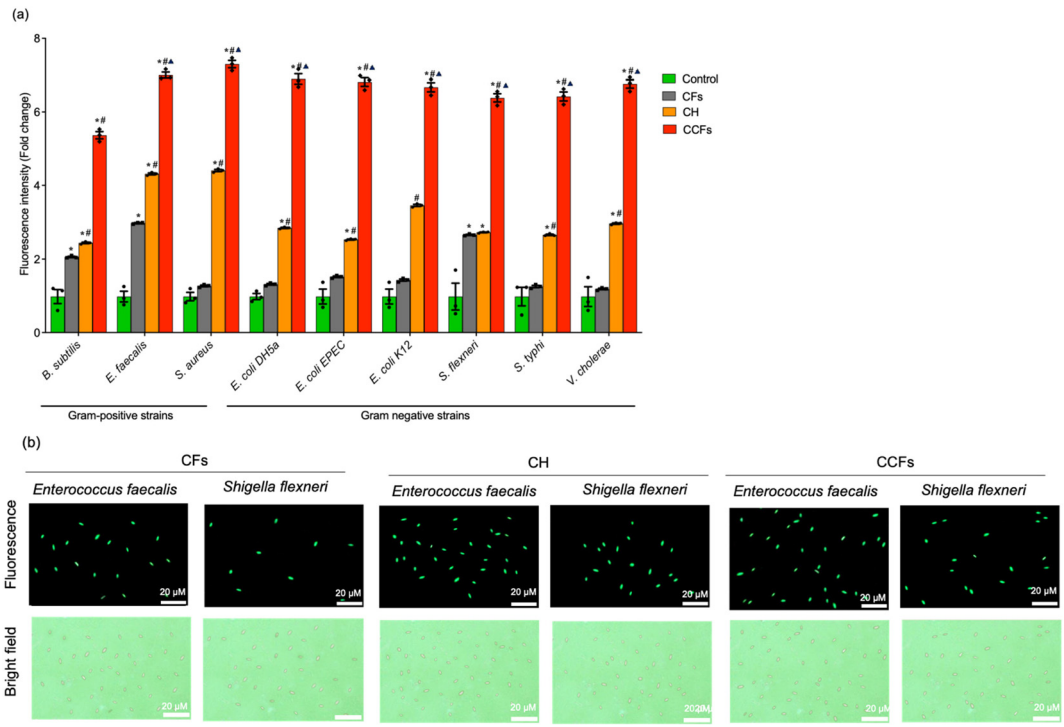

Fig. 2 CellTox™ Green uptake assay confirms CH or CCFs damage the bacterial membrane. Bacteria were treated with CFs, CH, and CCFs, and the fluorescence intensity was measured at 490 nm (a). The values presented are mean ± SEM (n = 3). Data were analysed using a one-way ANOVA coupled with a Bonferroni *post-hoc* test. *Significantly different from untreated control, *$p < 0.05$; # Significantly different from CFs, #$p < 0.05$ and ▲ significantly different from CH, ▲ $p < 0.05$. Bright field and white field image of CH, CFs, and CCFs (b). CFs: cobalt ferrite nanoparticles, CH: chitosan, CCFs: chitosan-coated cobalt ferrite nanoparticles.

branes. After CF internalization, ROS can be generated *via* the Fenton reaction and oxidize membrane polyunsaturated fatty acids.[41] Membrane LPO can disrupt the integrity of the cell membrane (Fig. 3b).[27] Additionally, ROS-mediated oxidative stress disrupts the electron transport chain and alters bacterial metabolic processes. Such disruptions can trigger the expression of apoptotic genes and oxidative stress-related proteins, ultimately leading to bacterial cell apoptosis.[42,43]

3.5 *In vitro* hemolytic activity

In vivo application of nanocomplexes requires excellent blood compatibility, including minimal hemolytic activity.[14] Due to ethical concerns surrounding the direct human exposure without prior animal studies, we evaluated the blood compatibility of CH, CFs, and CCFs using HRBCs and RRBCs to predict their potential effects *in vivo*

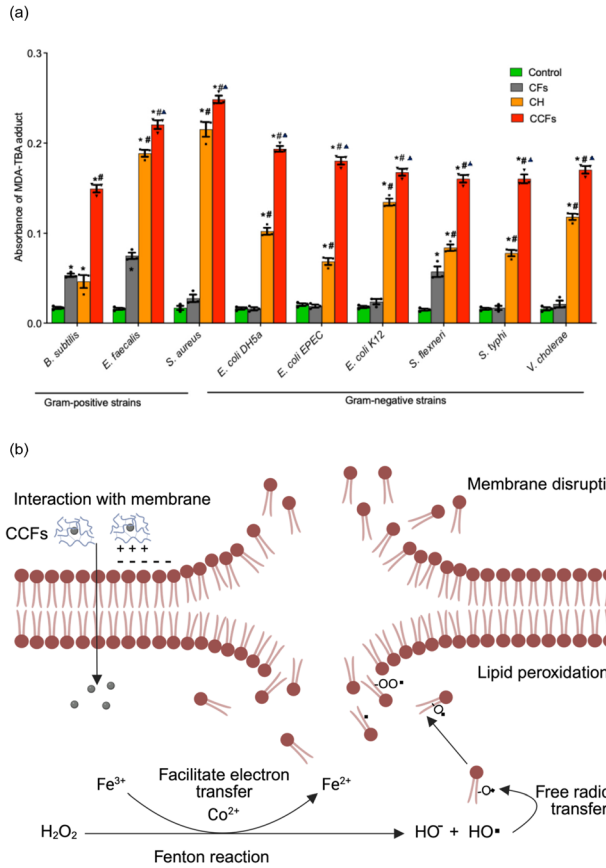

Fig. 3 Lipid peroxidation of the bacterial membrane and proposed mechanism of antibacterial activity. Bacteria were treated with CFs, CH and CCFs, and the MDA-TBA adduct was measured using a UV-vis spectrophotometer at 532 nm (a). The values presented are mean ± SEM (n = 3). Data were analysed using a one-way ANOVA coupled with a Bonferroni *post-hoc* test. *Significantly different from untreated control, *$p < 0.05$; #Significantly different from CFs, #$p < 0.05$ and ▲ significantly different from CH, ▲ $p < 0.05$. Proposed mechanism of the antimicrobial activity of CCFs (b). Positively charged CCFs interact with the negatively charged bacterial membrane, leading to membrane destabilization and increased permeability. This interaction also facilitates CFs' release from CCFs. Following CF internalization, ROS can be produced *via* the Fenton reaction and induce membrane LPO. CFs: cobalt ferrite nanoparticles, CH: chitosan, CCFs: chitosan-coated cobalt ferrite nanoparticles, MDA-TBA: malondialdehyde-thiobarbituric acid. The mechanistic scheme in (b) was drawn using BioRender (https://www.biorender.com).

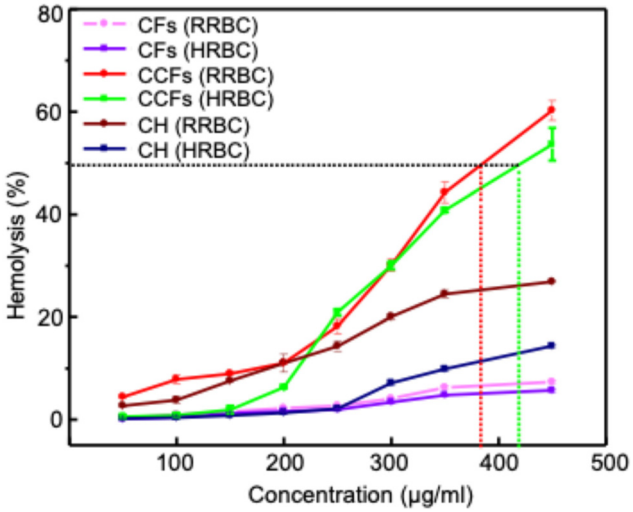

Fig. 4 Hemocompatibility of CFs, CH, and CCFs with human and rat red blood cells. The HC_{50} values of CCF for HRBCs and RRBCs were 383 and 420 μg mL^{-1}, respectively. The values presented are mean ± SEM (n = 3). HRBC: human red blood cells, RRBC: rat red blood cell, CFs: cobalt ferrite nanoparticles, CH: chitosan, CCFs: chitosan-coated cobalt ferrite nanoparticles.

(Fig. 4). Lee *et al.*[44] reported that acetylated CH nanoparticles exhibit negligible hemolytic activity, which can vary with their chemical modifications. In our study, CCFs induced higher hemolytic activity in both HRBCs and RRBCs compared to pristine CFs, likely due to differences in particle distribution and interaction with RBCs. While CFs tended to aggregate and precipitate at the bottom of the tube, CCFs remained homogeneously dispersed with altered particle size and surface area. RRBC membrane integrity was affected differently from that of HRBC with increasing concentrations of the test samples. These observations are consistent with the model proposed by Thomassen *et al.*,[45] in which RBC membranes locally induce curvature and exhibit reduced adhesion energy upon interaction with aggregated nanoparticles, resulting in lower hemolytic activity compared with monodispersed particles of the same size. Additionally, particle size and surface area contribute significantly to hemolysis.[46] Interestingly, CCFs showed higher cytotoxicity toward RRBCs than HRBCs in terms of HC_{50} values, which is less than the amount (500 μg) that exhibits the highest antibacterial activity against *S. aureus* (Fig. 4). *In vivo* studies also indicated that CCFs are well tolerated by RRBCs at lower concentrations.[26] Given the observed *in vitro* toxicity at higher concentrations, establishing a safe therapeutic window for CCFs is essential before considering direct human applications.

4. Conclusion

CCFs exhibited potent antimicrobial activity against both Gram-positive and Gram-negative bacteria, outperforming CH and CFs alone, as shown by larger zones of inhibition, lower MICs, and enhanced cytotoxicity in the CellTox™ Green assay. Among other bacterial strains, *Staphylococcus aureus* was the most susceptible strain, while LPO studies suggested that oxidative membrane damage is involved in the bactericidal mechanism. Overall, CH functionalization is an effective strategy for improving the antimicrobial performance of CFs. However, the hemolytic activity of CCFs is concentration-dependent, underscoring the need for careful dose optimization. Further work should, therefore, focus on defining a safe therapeutic window, establishing the behavior of these nanocomplexes in physiologically relevant systems, and validating their efficacy *in vivo*.

Author contributions

Conceptualization: M. S. S., M. A. H, and S. R. S; nanoparticle synthesis: M. S. S. and S. M. H.; antimicrobial and hemolysis activity: M. S. S., S. A. P., M. M. H, and M. S. N.; microscopic analysis: M. M. H.; data analysis and diagram: M. S. S., S. A. P., and M. M. H.; manuscript writing: M. S. S. and S. A. P.; manuscript revision and approval: M. S. S., M. A. H., and S. R. S.

Ethics statement

All animal procedures were performed in accordance with the Guidelines for Care and Use of Laboratory Animals of Jahangirnagar University and experiments were approved by the Animal Ethics Committee of the Biosafety, Biosecurity & Ethical Committee, Faculty of Biological Sciences, Jahangirnagar (Ref. No: BBEC, JU/M 2018 (11) 1).

All experiments were performed in accordance with the Guidelines of Jahangirnagar University, and Experiments were approved by the ethics committee at the Biosafety, Biosecurity & Ethical Committee, Faculty of Biological Sciences, Jahangirnagar University (Ref. No: BBEC, JU/M 2019 (4) 1). Informed consent was obtained from the human participants of this study.

Conflicts of interest

There are no conflicts to declare.

Data availability

Data are included in the article or in the supplementary information (SI). Supplementary information: Table S1: Characterization parameters of CFs, CH and CCFs. Table S2: MIC of CCFs, CH and CFs against bacteria. Fig. S1: Trypan blue dye exclusion assay showing CH, CF, and CCF induced bacterial cell wall damage. See DOI: https://doi.org/10.1039/d6pm00045b.

Acknowledgements

Jahangirnagar University Research Grant 2019, and University Grants Commission (UGC)-Jahangirnagar University Joint Research Grant 2019, Government of Bangladesh, provided partial funding for this research project. The authors are thankful to Wazed Mia Science Research Centre, Jahangirnagar University, for allowing the use of their microscope facilities.

References

1 A. Azam, A. S. Ahmed, M. Oves, M. S. Khan, S. S. Habib and A. Memic, Antimicrobial activity of metal oxide nanoparticles against Gram-positive and Gram-negative bacteria: a comparative study, *Int. J. Nanomed.*, 2012, **7**, 6003–6009.

2 B. Aslam, W. Wang, M. I. Arshad, M. Khurshid, S. Muzammil, M. H. Rasool, M. A. Nisar, R. F. Alvi, M. A. Aslam, M. U. Qamar, M. K. F. Salamat and Z. Baloch, Antibiotic resistance: A rundown of a global crisis, *Infect. Drug Resist.*, 2018, **11**, 1645–1658.

3 X. Li, S. M. Robinson, A. Gupta, K. Saha, Z. Jiang, D. F. Moyano, A. Sahar, M. A. Riley and V. M. Rotello, Functional gold nanoparticles as potent antimicrobial agents against multi-drug-resistant bacteria, *ACS Nano*, 2014, **8**(10), 10682–10686.

4 R. Barnett, Typhoid fever, *Lancet*, 2016, **388**(10059), 2467.

5 K. V. Singh, S. R. Nallapareddy and B. E. Murray, Importance of the ebp (endocarditis- and biofilm-associated pilus) locus in the pathogenesis of *Enterococcus faecalis* ascending urinary tract infection, *J. Infect. Dis.*, 2007, **195**(11), 1671–1677.

6 T. J. Ochoa and C. A. Contreras, Enteropathogenic *Escherichia coli* infection in children, *Curr. Opin. Infect. Dis.*, 2011, **24**(5), 478–483.

7 S. Y. Tong, J. S. Davis, E. Eichenberger, T. L. Holland and V. G. Fowler, Jr., *Staphylococcus aureus* infections: Epidemiology, pathophysiology, clinical manifestations, and management, *Clin. Microbiol. Rev.*, 2015, **28**(3), 603–661.

8 A. V. Jennison and N. K. Verma, *Shigella flexneri* infection: Pathogenesis and vaccine development, *FEMS Microbiol. Rev.*, 2004, **28**(1), 43–58.

9 E. J. Nelson, J. B. Harris, J. G. Morris, Jr., S. B. Calderwood and A. Camilli, Cholera transmission: The host, pathogen and bacteriophage dynamic, *Nat. Rev. Microbiol.*, 2009, **7**(10), 693–702.

10 A. C. Rios, C. G. Moutinho, F. C. Pinto, F. S. Del Fiol, A. Jozala, M. V. Chaud, M. M. Vila, J. A. Teixeira and V. M. Balcão, Alternatives to overcoming bacterial resistances: State-of-the-art, *Microbiol. Res.*, 2016, **191**, 51–80.

11 Y. N. Slavin, J. Asnis, U. O. Häfeli and H. Bach, Metal nanoparticles: Understanding the mechanisms behind antibacterial activity, *J. Nanobiotechnol.*, 2017, **15**(1), 65.

12 S. H. Hussein-Al-Ali, M. E. El Zowalaty, M. Z. Hussein, B. M. Geilich and T. J. Webster, Synthesis, characterization, and antimicrobial activity of an ampicillin-conjugated magnetic nanoantibiotic for medical applications, *Int. J. Nanomed.*, 2014, **9**, 3801–3814.

13 A. Ashour, A. I. El-Batal, M. A. Maksoud, G. S. El-Sayyad, S. Labib, E. Abdeltwab and M. El-Okr, Antimicrobial activity of metal-substituted cobalt ferrite nanoparticles synthesized by sol–gel technique, *Particuology*, 2018, **40**, 141–151.

14 H. Wu, G. Liu, X. Wang, J. Zhang, Y. Chen, J. Shi, H. Yang, H. Hu and S. Yang, Solvothermal synthesis of cobalt ferrite nanoparticles loaded on multiwalled carbon nanotubes for magnetic resonance imaging and drug delivery, *Acta Biomater.*, 2011, **7**(9), 3496–3504.

15 F. Ahmad and Y. Zhou, Pitfalls and challenges in nanotoxicology: A case of cobalt ferrite (CoFe2O4) nanocomposites, *Chem. Res. Toxicol.*, 2017, **30**(2), 492–507.

16 S. K. Shukla, A. K. Mishra, O. A. Arotiba and B. B. Mamba, Chitosan-based nanomaterials: A state-of-the-art review, *Int. J. Biol. Macromol.*, 2013, **59**, 46–58.
17 A. Rafique, K. Mahmood Zia, M. Zuber, S. Tabasum and S. Rehman, Chitosan functionalized poly(vinyl alcohol) for prospects biomedical and industrial applications: A review, *Int. J. Biol. Macromol.*, 2016, **87**, 141–154.
18 W. Rao, H. Wang, J. Han, S. Zhao, J. Dumbleton, P. Agarwal, W. Zhang, G. Zhao, J. Yu, D. L. Zynger, X. Lu and X. He, Chitosan-decorated doxorubicin-encapsulated nanoparticle targets and eliminates tumor reinitiating cancer stem-like cells, *ACS Nano*, 2015, **9**(6), 5725–5740.
19 D. Gingasu, I. Mindru, L. Patron, A. Ianculescu, E. Vasile, G. Marinescu, S. Preda, L. Diamandescu, O. Oprea and M. Popa, Synthesis and characterization of chitosan-coated cobalt ferrite nanoparticles and their antimicrobial activity, *J. Inorg. Organomet. Polym. Mater.*, 2018, **28**(5), 1932–1941.
20 C. I. Covaliu, I. Jitaru, G. Paraschiv, E. Vasile, S.-Ş. Biriş, L. Diamandescu, V. Ionita and H. Iovu, Core–shell hybrid nanomaterials based on $CoFe_2O_4$ particles coated with PVP or PEG biopolymers for applications in biomedicine, *Powder Technol.*, 2013, **237**, 415–426.
21 V. Umaiya Bharathi and S. Thambidurai, Bio-fabrication of chitosan-coated cobalt oxide nanocomposite for enhanced bacterial inhibition and oxidative stress mitigation, *Chem. Phys. Lett.*, 2024, **855**, 141561.
22 D. G. Guedes, G. G. Guedes, J. d. O. d. Silva, A. L. d. Silva, C. B. B. Luna, B. P. G. d. L. Damasceno and A. C. F. d. M. Costa, Development of scaffolds with chitosan magnetically activated with cobalt nanoferrite: A study on physical–chemical, mechanical, cytotoxic and antimicrobial behavior, *Pharmaceuticals*, 2024, **17**(10), 1332.
23 L. Doan, A. H. Huynh, K. Tran, Q. N. Le and K. G. Huynh, Surface modifications of cobalt ferrites nanoparticles with chitosan, polyethylene glycol, polyvinyl alcohol, and polyvinylpyrrolidone as antibacterial agents against *Staphylococcus aureus*, *Pseudomonas aeruginosa*, and *Salmonella enterica*, *Polyhedron*, 2025, **267**, 117354.
24 M. Ganan, A. V. Carrascosa and A. J. Martínez-Rodríguez, Antimicrobial activity of chitosan against *Campylobacter* spp. and other microorganisms and its mechanism of action, *J. Food Prot.*, 2009, **72**(8), 1735–1738.
25 Y. J. Jing, Y. J. Hao, H. Qu, Y. Shan, D. S. Li and R. Q. Du, Studies on the antibacterial activities and mechanisms of chitosan obtained from cuticles of housefly larvae, *Acta Biol. Hung.*, 2007, **58**(1), 75–86.
26 M. S. Shakil, M. A. Hasan, M. F. Uddin, A. Islam, A. Nahar, H. Das, M. N. I. Khan, B. P. Dey, B. Rokeya and S. M. Hoque, In vivo toxicity studies of chitosan-coated cobalt ferrite nanocomplex for its application as MRI contrast dye, *ACS Appl. Bio Mater.*, 2020, **3**(11), 7952–7964.
27 M. S. Niloy, M. M. Hossain, M. Takikawa, M. S. Shakil, S. A. Polash, K. M. Mahmud, M. F. Uddin, M. Alam, R. D. Shubhra, M. M. A. K. Shawan, T. Saha, S. Takeoka, M. A. Hasan and S. Ranjan Sarker, Synthesis of biogenic silver nanoparticles using *Caesalpinia digyna* and investigation of their antimicrobial activity and in vivo biocompatibility, *ACS Appl. Bio Mater.*, 2020, **3**(11), 7722–7733.
28 R. Mondal, S. A. Polash, T. Saha, Z. Islam, M. M. Sikder, N. Alam, M. S. Hossain and S. R. Sarker, Investigation of the phytoconstituents and bioactivity of various parts of wild type and cultivated *Phyllanthus emblica* L, *Adv. Biosci. Biotechnol.*, 2017, **8**, 211–227.
29 W. Strober, Trypan blue exclusion test of cell viability, *Curr. Protoc. Immunol.*, 2001, Appendix 3, Appendix 3B.
30 M. M. Hossain, S. A. Polash, M. Takikawa, R. D. Shubhra, T. Saha, Z. Islam, S. Hossain, M. A. Hasan, S. Takeoka and S. R. Sarker, Investigation of the antibacterial activity and in vivo cytotoxicity of biogenic silver nanoparticles as potent therapeutics, *Front. Bioeng. Biotechnol.*, 2019, **7**, 239.
31 S. Ranjan Sarker, S. A. Polash, J. Boath, A. E. Kandjani, A. Poddar, C. Dekiwadia, R. Shukla, Y. Sabri and S. K. Bhargava, Functionalization of elongated tetrahexahedral au nanoparticles and their antimicrobial activity assay, *ACS Appl. Mater. Interfaces*, 2019, **11**(14), 13450–13459.
32 J. H. Zhang, T. D. Chung and K. R. Oldenburg, A simple statistical parameter for use in evaluation and validation of high throughput screening assays, *J. Biomol. Screening*, 1999, **4**(2), 67–73.
33 M. Hossain, S. A. Polash, M. Takikawa, R. D. Shubhra, T. Saha, Z. Islam, S. Hossain, M. Hasan, S. Takeoka and S. R. Sarker, Investigation of the antibacterial activity and in vivo cytotoxicity of biogenic silver nanoparticles as potent therapeutics, *Front. Bioeng. Biotechnol.*, 2019, **7**, 239.
34 A. A. Kajani, A. Pouresmaeili and M. Kamali, Facile one-pot synthesis of the mesoporous chitosan-coated cobalt ferrite nanozyme as an antibacterial and MRI contrast agent, *RSC Adv.*, 2024, **14**(24), 16801–16808.
35 D. Şen Karaman, S. Sarwar, D. Desai, E. M. Björk, M. Odén, P. Chakrabarti, J. M. Rosenholm and S. Chakraborti, Shape engineering boosts antibacterial activity of chitosan coated mesoporous silica nanoparticle doped with silver: a mechanistic investigation, *J. Mater. Chem. B*, 2016, **4**(19), 3292–3304.
36 M. Bittremieux, K. Mikoshiba and G. Bultynck, Data on cytotoxicity in HeLa and SU-DHL-4 cells exposed to DPB162-AE compound, *Data Brief*, 2017, **12**, 91–96.
37 S. A. Polash, M. M. Hossain, T. Saha and S. R. Sarker, Biogenic silver nanoparticles: A potent therapeutic agent, in *Emerging Trends in Nanomedicine*, ed. S. Singh, Springer Singapore, Singapore, 2021, pp. 81–127.
38 S. Ranjan Sarker, S. A. Polash, J. Boath, A. E. Kandjani, A. Poddar, C. Dekiwadia, R. Shukla, Y. Sabri and S. K. Bhargava, Functionalization of elongated tetrahexahedral Au nanoparticles and their antimicrobial activity assay, *ACS Appl. Mater. Interfaces*, 2019, **11**(14), 13450–13459.
39 R. Torres-Mendieta, N. H. A. Nguyen, A. Guadagnini, J. Semerad, D. Łukowiec, P. Parma, J. Yang, S. Agnoli, A. Sevcu, T. Cajthaml, M. Cernik and V. Amendola, Growth suppression of bacteria by biofilm deterioration using silver nanoparticles with magnetic doping, *Nanoscale*, 2022, **14**(48), 18143.

40 T. Dörr, P. J. Moynihan and C. Mayer, Editorial: Bacterial cell wall structure and dynamics, *Front. Microbiol.*, 2019, **10**, 2051.
41 N. T. Tasnim, N. Ferdous, M. M. H. Rumon and M. S. Shakil, The promise of metal-doped iron oxide nanoparticles as antimicrobial agent, *ACS Omega*, 2024, **9**(1), 16–32.
42 L. Wang, C. Hu and L. Shao, The antimicrobial activity of nanoparticles: present situation and prospects for the future, *Int. J. Nanomed.*, 2017, **12**, 1227.
43 H.-J. Park, J. Y. Kim, J. Kim, J.-H. Lee, J.-S. Hahn, M. B. Gu and J. Yoon, Silver-ion-mediated reactive oxygen species generation affecting bactericidal activity, *Water Res.*, 2009, **43**(4), 1027–1032.
44 D.-W. Lee, K. Powers and R. Baney, Physicochemical properties and blood compatibility of acylated chitosan nanoparticles, *Carbohydr. Polym.*, 2004, **58**(4), 371–377.
45 L. C. Thomassen, V. Rabolli, K. Masschaele, G. Alberto, M. Tomatis, M. Ghiazza, F. Turci, E. Breynaert, G. Martra, C. E. Kirschhock, J. A. Martens, D. Lison and B. Fubini, Model system to study the influence of aggregation on the hemolytic potential of silica nanoparticles, *Chem. Res. Toxicol.*, 2011, **24**(11), 1869–1875.
46 Y. Zhao, X. Sun, G. Zhang, B. G. Trewyn, I. I. Slowing and V. S. Lin, Interaction of mesoporous silica nanoparticles with human red blood cell membranes: size and surface effects, *ACS Nano*, 2011, **5**(2), 1366–1375.